









[View Journal Online](#)
[View Article Online](#)

Synthesis, X-ray structure, and DFT analysis of a binary complex of 3,3'-[(3-benzimidazolyl)methylene]bis(4-hydroxy-2H-1-benzopyran-2-one): 5-Methyl-1,3-thiazol-2(3H)-imine

Gopal Sharma ¹, Anshul Uppal ¹, Sumati Anthal ¹, Madhukar Baburao Deshmukh ²,
 Priyanka Pandharinath Mohire ², Tanaji Ramchandra Bhosale ²,
 Chellappanpillai Sudarsanakumar ³ and Rajni Kant ^{1,*}

¹X-ray Crystallography Laboratory, Department of Physics, University of Jammu, Jammu Tawi, 180006, India

gopalgulshan1992@gmail.com (G.S.), anshulupp629@gmail.com (A.U.), sumatiantal@gmail.com (S.A.), rkantju@gmail.com (R.K.)

²Department of Chemistry, Shivaji University, Kolhapur, 416004, India

m_deshmukh1@rediffmail.com (M.B.D.), mohire.priyanka258@gmail.com (P.P.M.), trbhosale2013@gmail.com (T.R.B.)

³School of Pure and Applied Physics, Mahatma Gandhi University, Kerala, 686560, India

c.sudarsan.mgu@gmail.com (C.S.)

* Corresponding author at: X-ray Crystallography Laboratory, Department of Physics, University of Jammu, Jammu Tawi, 180006, India.

e-mail: rkantju@gmail.com (R. Kant).

RESEARCH ARTICLE

ABSTRACT



doi 10.5155/eurjchem.11.4.324-333.2028

Received: 18 August 2020

Received in revised form: 16 October 2020

Accepted: 22 October 2020

Published online: 31 December 2020

Printed: 31 December 2020

KEYWORDS

DFT

Direct methods

X-ray diffraction

Crystal structure

Benzopyran derivatives

Intermolecular interactions

A combined theoretical and experimental investigation on a pharmaceutically important binary complex 3,3'-[(3-benzimidazolyl)methylene]bis(4-hydroxy-2H-1-benzopyran-2-one): 5-methyl-1,3-thiazol-2(3H)-imine is presented in this manuscript. The compound crystallizes in the monoclinic crystal system with space group *Cc* with unit cell parameters: $a = 19.8151(8)$ Å, $b = 15.2804(6)$ Å, $c = 8.3950(4)$ Å, $\beta = 94.0990(10)^\circ$, $V = 2535.36(19)$ Å³, $Z = 4$, $T = 296(2)$ K, $\mu(\text{MoK}\alpha) = 0.184$ mm⁻¹, $D_{\text{calc}} = 1.490$ g/cm³, 35833 reflections measured ($5.332^\circ \leq 2\theta \leq 56.678^\circ$), 6168 unique ($R_{\text{int}} = 0.0467$, $R_{\text{sigma}} = 0.0388$) which were used in all calculations. The final R_1 was 0.0435 ($I > 2\sigma(I)$) and wR_2 was 0.1073 (all data). The crystal structure has been determined by the conventional X-ray diffraction method, solved by direct methods and refined by the full matrix least squares procedure. Intramolecular hydrogen bonding of the type C-H...O and O-H...O is present and the crystal structure stabilizes via N-H...O, C-H...N and O-H...N intermolecular interactions. The optimized structural parameters have been compared and the parameters like ionization potential, electron affinity, global hardness, electron chemical potential, electronegativity, and global electrophilicity based on HOMO and LUMO energy values were calculated at B3LYP/6-311G(d,p) level of theory for a better understanding of the structural properties of the binary complex.

Cite this: *Eur. J. Chem.* 2020, 11(4), 324-333

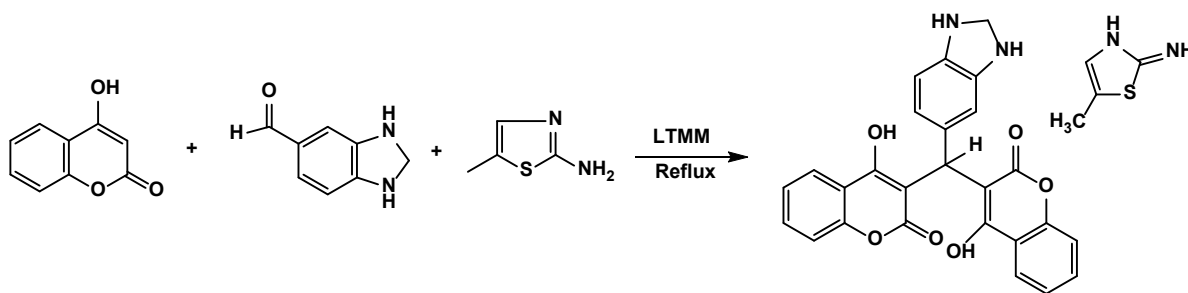
Journal website: www.eurjchem.com

1. Introduction

Coumarin derivatives, i.e., molecules containing the benzopyran-2-one or chromen-2-one ring system, are widely distributed throughout nature, occurring as secondary metabolites of plant species, notably in the tonka bean and Melilotus species [1]. Natural coumarins play an important role in plant biochemistry and physiology and act as antioxidants, enzyme inhibitors, and precursors of toxic substances [2]. These are also involved in the actions of plant growth hormones and growth regulators, the control over respiration and photosynthesis, as well as in the defense against various infections [3]. Substitutions on the benzopyrone ring influence the chemical, structural [4], and biological properties of coumarins [5-7]. Coumarin heterocyclic derivatives exhibit diverse biological activities, as reviewed recently [8]. The biological activities of coumarin derivatives, in particular their

therapeutic application as antifungal, antibacterial [9], anti-tubercular [10], antiacetylcholinesterase, anticancer [11,12] anticoagulant, antimutagenic, anti-hepatites C, anti-inflammatory [13], and analgesic [14] agents. Moreover, many coumarin derivatives are used as non-peptidic proteases [15], heat shock proteins [16,17], and monoamine oxidase [18]. The interest in coumarins has recently increased significantly because it was found that they inhibit HIV (human immunodeficiency virus), by affecting integrase and reverse transcriptase, which play a critical role in the replicative cycle of HIV [19-21].

Compounds containing a thiazole ring are known to have versatile pharmacological roles [22]. Substituted benzimidazoles also possess many biological activities, which is why benzimidazole derivatives are considered as an important moiety for the development of molecules of pharmaceutical interest [23,24].



Scheme 1. Reaction scheme of 3,3'-[(3-benzimidazolyl)methylene]bis(4-hydroxy-2H-1-benzopyran-2-one):5-methyl-1,3-thiazol-2(3H)-imine.

With the importance of both coumarin and thiazole pharmaceuticals in mind, we were interested in developing a synthetic route to a binary complex that contains both entities with the aim of exploring whether or not the effects of the two units would work in concert in a pharmaceutical sense in the combined molecules [4,25].

The present study is focused on synthesis, X-ray structure, and DFT analysis of a binary complex of 3,3'-[(3-benzimidazolyl)methylene]bis(4-hydroxy-2H-1-benzopyran-2-one):5-methyl-1,3-thiazol-2(3H)-imine. Studies on single crystal structure, crystal packing, molecular electrostatic potential map, and HOMO-LUMO plots provide supportive information about the crystal. The calculated optimized structural parameters were compared and the parameters like ionization potential, electron affinity, global hardness, electron chemical potential, electronegativity, and global electrophilicity based on HOMO and LUMO energy values were calculated at B3LYP/6-311G(d,p) level of theory for a better understanding of the structural properties.

2. Experimental

2.1. Materials and instrumentations

All chemicals were purchased from Alfa Aesar and Spectrochem (PVT. Ltd, Mumbai, India), Sigma Aldrich and used without purification. The reaction was monitored by TLC. The desired structures of the synthesized compounds were confirmed by their relevant spectral data. The melting points were determined by the open glass capillary method and are uncorrected. The compounds were confirmed by IR and ^1H NMR spectral data. The IR spectra were recorded on a JASCO FT-IR spectrophotometer (FTIR-4600) and the values are expressed as ν_{max} (cm^{-1}). The ^1H NMR spectra were recorded on Bruker Avance II 300 MHz using $\text{DMSO}-d_6$ as a solvent and TMS as an internal standard.

2.2. Synthesis of 3,3'-[(3-benzimidazolyl)methylene]bis(4-hydroxy-2H-1-benzopyran-2-one):5-methyl-1,3-thiazol-2(3H)-imine

A mixture of 4-hydroxycoumarin (1 mmole) and dihydro benzimidazole 5-carbaldehyde (1 mmole), with 5 mL low transition temperature mixture was taken in a 50 mL round bottomed flask at room temperature to form the Knoevenagel condensation product, monitored by TLC and then 2-amino 5-methyl thiazole (1 mmole) was added and the same reaction mixture refluxed for 20 min. The 2-amino 5-methyl thiazole is not involved in the Knoevenagel condensation, however, it forms a conglomerate with the chiral product formed by the condensation of two molecules of 4-hydroxy coumarin with 5-formyl dihydrobenzimidazole which separates in the form of transparent crystals. The progress of the reaction was monitored by TLC using petroleum ether:ethyl acetate (8:2, v:v). After the completion of the reaction, the mixture was

cooled to room temperature and the product collected by simple filtration, washed with ethanol and diethyl ether. Finally, the crude product was recrystallized from ethanol to obtain the pure product. The Reaction scheme of the title compound is shown in Scheme 1.

3,3'-[(3-Benzimidazolyl)methylene] bis(4-hydroxy-2H-1-benzopyran-2-one):5-Methyl-1,3-thiazol-2(3H)-imine: Yield: 60%. M.p. 208-210 °C. FT-IR (KBr, ν , cm^{-1}): 3300-3150(NH), 2930(C-H), 1670 (C=O), 1605 (C=C). ^1H NMR (300 MHz, $\text{DMSO}-d_6$, δ , ppm): 2.1 (s, 3H, CH_3), 3.8 (d, 2H, CH_2), 4.6 (t, 2H, 2×NH of imidazole ring), 4.8 (s, 1H, NH of thiazole ring), 6.25 (s, 1H, CH benzylic proton), 6.8-8.1 (m, 12H, Aromatic protons & proton of thiazole ring), 8.6 (s, 1H, C=NH), 14.5 (s br, 2H, 2×OH enolic).

2.3. Crystal structure determination and refinement

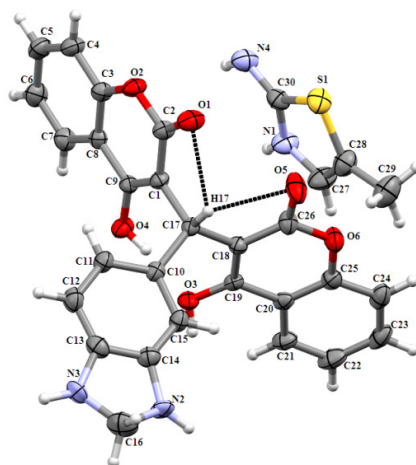
X-ray intensity data of the crystal of dimensions $0.25 \times 0.30 \times 0.35 \text{ mm}^3$ were collected on a Bruker APEX-II CCD area detector diffractometer [26] equipped with graphite monochromated $\text{MoK}\alpha$ radiation ($\lambda = 0.71073 \text{ \AA}$). The data were collected at 296(2) K and 6168 reflections were found as unique. The intensities were measured by ϕ/ω scan mode for θ range 2.67 to 27.46°. A total of 4717 reflections with $I > 2\sigma(I)$ were treated as observed. Data was corrected for Lorentz-polarization and absorption factors. The structure was solved by direct methods using SHELXS [27] and was refined using SHELXL [28]. All non-hydrogen atoms of the binary complex were located from the best E-map. All hydrogen atoms were geometrically fixed (except N4 hydrogen atom) and allowed to ride on their parent carbon atoms with C-H = 0.93-0.97 Å, N-H = 0.86 Å. The final refinement cycles converged to an R-factor of 0.044 and $wR(F^2) = 0.107$ for 4717 observed reflections. The residual electron density ranges from -0.32 to 0.28 $\text{e}\cdot\text{\AA}^{-3}$. The geometry of the binary complex was calculated using the WinGX [29], PARST [30], and PLATON [31] software. Crystallographic information file (CIF) has been deposited at the Cambridge Crystallographic Data Centre with CCDC-1948179. A precise description of the crystallographic data of the X-ray structure is given in Table 1.

2.4. Theoretical calculation

The optimized structure of the compound 3,3'-[(3-benzimidazolyl)methylene]bis(4-hydroxy-2H-1-benzopyran-2-one):5-methyl-1,3-thiazol-2(3H)-imine has been obtained by using Hartree-Fock (HF) method and is the same got re-optimized by using Becke's three-parameter hybrid function (B3) [32,33] for the exchange part and the Lee-Yang-Parr (LYP) correlation function [34] using 6-311G basis set. The natural bond orbital (NBO) analyses, frontier molecular orbitals, atomic charges, and molecular electrostatic potential surface calculations were carried out by using Gaussian 09W [35] program.

Table 1. Crystal data and experimental details.

Empirical formula	C ₂₆ H ₁₈ N ₂ O ₆ ·C ₄ H ₆ N ₂ S
Formula weight	568.59
Temperature (K)	296(2)
Crystal system	Monoclinic
Space group	Cc
a (Å)	19.8151(8)
b (Å)	15.2804(6)
c (Å)	8.3950(4)
β (°)	94.0990(10)
Volume (Å ³)	2535.36(19)
Z	4
ρ _{calc} (g/cm ³)	1.490
μ (mm ⁻¹)	0.184
F(000)	1184.0
Crystal size (mm ³)	0.350 × 0.300 × 0.250
Radiation	MoKα (λ = 0.71073)
2θ range for data collection (°)	5.332 to 56.678
T _{min} , T _{max}	0.938, 0.955
Index ranges	-25 ≤ h ≤ 26, -20 ≤ k ≤ 20, -11 ≤ l ≤ 10
Reflections collected	35833
Independent reflections	6168 [R _{int} = 0.0467, R _{sigma} = 0.0388]
Data/restraints/parameters	6168/2/379
Goodness-of-fit on F ²	1.021
Final R indexes [I ≥ 2σ (I)]	R ₁ = 0.0435, wR ₂ = 0.0967
Final R indexes [all data]	R ₁ = 0.0700, wR ₂ = 0.1073
Largest diff. peak/hole (e Å ⁻³)	0.28/-0.32
Flack parameter	0.03(10)
CCDC Number	1948179

**Figure 1.** ORTEP view of the binary complex with displacement ellipsoids drawn at 40% probability level.

3. Results and discussion

3.1. Single crystal structure analysis

The structure containing atom numbering scheme is shown in Figure 1 [36]. The bond distances, bond angles which play an important role in collating the structural properties of the binary complex with the related structures are presented in Table 2. The values of bond distance [37] and angles of all the rings are within the normal range. The C2-O1 = 1.213 Å and C26-O5 = 1.211 Å bond distances of the title compound are comparable with the values observed for some analogous structure [38,39]. In fact, the distances C9-O4 = 1.310 Å and C19-O3 = 1.295 Å is smaller than the values observed for some analogous structure [38,39]. The bond angles O1-C2-O2 = 114.7(3)°, O1-C2-C1 = 127.0(3)°, O5-C26-O6 = 114.0(3)° and O5-C26-C18 = 126.8(3)° are comparable with the values observed in some related structure. The atoms in the coumarin moiety deviate slightly from the planarity maximum deviation observed for C1 [-0.0342] and C23 [-0.0693] atoms. The imidazole ring in the molecule adopts an envelope conformation with a single mirror plane of symmetry passing through the C13-C14 bond (asymmetry parameter ΔC_s = 0.474).

The packing of the molecules in the unit cell is governed by both the intra and intermolecular interactions. In the crystal structure, adjacent molecules are interconnected through N1-H1...O1, N1-H1...O5, N4-H4A...O1, C23-H23...N2 and O3-H3A...N4 intermolecular hydrogen bonds. Here, the atoms O1, O5, N2, and N4 and nitrogen atom N1 of the five-membered thiazole ring act as hydrogen bond acceptors while the atoms N4, C23 and O3 act as hydrogen bond donors. In addition to the intermolecular hydrogen bonding network, C17-H17...O1, C17-H17...O5 and O4-H4C...O3 intramolecular interactions have also been observed which results in the formation of two (virtual five-membered rings) with a graph-set motif S(5) (Figure 1). The supramolecular assembly is formed by the intermolecular interactions of the type N-H...O and O-H...N which links the molecules to form a chain running parallel to *a*-axis, whereas hydrogen bond of the type C-H...N having atom C23 as the donor links the molecules to form a chain parallel to *b*-axis. The N1 atom of thiazole ring is the hydrogen bond donor that forms bifurcated hydrogen bonds with two different carbonyl groups [N1-H1...O1 (2.966 Å), N1-H1...O5 (2.724 Å) give rise to R₂¹(6) motif. Intermolecular hydrogen bonds of the type N-H...O and O-H...N are mainly responsible for stabilizing the crystal packing.

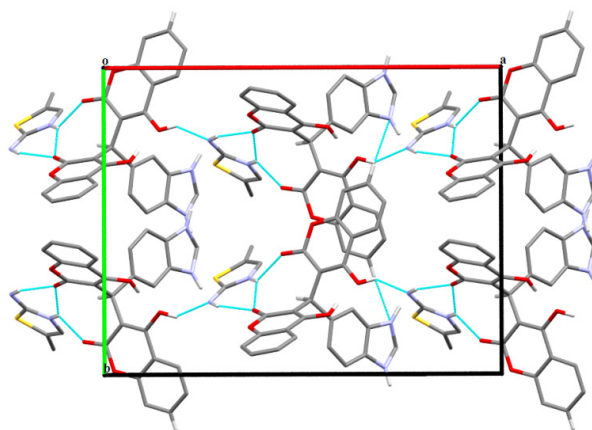
Table 2. Comparison between experimental and calculated selected bond lengths (Å) and bond angles (°) of C₂₆H₁₈N₂O₆-C₄H₆N₂S using HF and DFT/6-311G basis set.

Bond	Bond lengths			Bond	Bond lengths		
	Experimental	Calculated			Experimental	Calculated	
		HF/6-311G	DFT/6-311G			HF/6-311G	DFT/6-311G
C13-N3	1.387(5)	1.401	1.398	C26-O5	1.211(4)	1.212	1.234
C14-N2	1.387(5)	1.318	1.342	C26-O6	1.387(4)	1.370	1.421
C10-C17	1.533(4)	1.508	1.508	C19-O3	1.295(4)	1.339	1.349
N2-C16	1.425(5)	1.470	1.479	C25-O6	1.366(4)	1.368	1.387
C2-O2	1.375(4)	1.391	1.427	C28-C27	1.317(6)	1.323	1.343
C2-O1	1.213(4)	1.277	1.293	C28-S1	1.755(4)	1.845	1.856
C17-C1	1.526(5)	1.541	1.553	C28-C29	1.500(6)	1.488	1.489
C9-O4	1.310(4)	1.450	1.486	C27-N1	1.373(6)	1.387	1.393
C17-C18	1.527(5)	1.512	1.514	C30-N1	1.326(5)	1.361	1.374
C13-C14	1.367(6)	1.455	1.459	C30-S1	1.717(4)	1.845	1.890
C3-O2	1.369(4)	1.377	1.402	C30-N4	1.317(5)	1.267	1.285
N3-C16	1.418(6)	1.452	1.460				
Bond	Bond angles			Bond	Bond angles		
		HF/6-311G	DFT/6-311G			HF/6-311G	DFT/6-311G
S1-C28-C29	121.5(4)	120.3	120.5	C17-C18-C19	124.2(3)	127.9	127.5
C17-C1-C2	115.9(3)	129.3	128.5	C18-C19-O3	122.6(3)	123.9	123.8
C17-C1-C9	123.6(3)	104.0	104.0	O5-C26-C18	126.8(3)	125.1	126.2
C20-C19-O3	119.6(3)	114.7	115.2	O6-C26-O5	114.0(3)	117.0	115.8
C1-C2-O1	127.0(3)	129.4	130.1	C26-C18-C17	114.8(3)	113.1	112.5
O2-C2-O1	114.7(3)	111.9	111.0	C15-C10-C17	118.7(3)	127.8	127.4
C8-C9-O4	115.0(3)	109.2	109.4	C10-C17-C18	115.1(3)	117.3	118.8
C1-C9-O4	125.3(3)	111.9	111.5	C7-C8-C9	123.6(3)	121.8	121.4
C11-C10-C17	121.3(3)	108.2	109.1	C27-C28-C29	128.9(4)	130.5	130.0
O2-C3-C4	116.1(3)	116.5	116.2	O6-C25-C24	115.8(3)	118.1	117.7
S1-C30-N4	124.6(3)	128.3	129.0	N1-C30-N4	125.3(4)	124.6	124.6

Table 3. Hydrogen bonding geometry (e.s.d's in parentheses).

D-H...A	D-H (Å)	H...A (Å)	D...A (Å)	∠ D-H...A (°)
O4-H4C...O3	0.82	1.67	2.462(3)	162
C17-H17...O1	0.98	2.33	2.871(4)	114
C17-H17...O5	0.98	2.33	2.826(4)	110
N1-H1...O1 ⁱ	0.86	2.27	2.966(4)	138
N1-H1...O5 ⁱ	0.86	2.12	2.724(5)	127
N4-H4A...O1 ⁱ	0.83(5)	2.21(4)	2.956(4)	150(4)
C23-H23...N2 ⁱⁱ	0.93	2.58	3.468(5)	160
O3-H3A...N4 ⁱⁱⁱ	0.82	2.26	2.839(4)	128

Symmetry code: (i) 1/2 + x, 1/2 - y, -1/2 + z (ii) x, -y, -1/2 + z. (iii) x, y, z.

**Figure 2.** Packing of the molecules viewed down the c-axis.

The molecular packing in the unit cell as viewed down the c-axis is shown in Figure 2 [36] and the geometry of intra- and inter-molecular hydrogen bonds is given in Table 3.

3.2. Theoretical calculation

3.2.1. Molecular geometry

The optimized structure of 3,3'-[(3-benzimidazolyl)methylene]bis(4-hydroxy-2H-1-benzopyran-2-one):5-methyl-1,3-thiazol-2(3H)-imine is shown in Figure 3. The optimized geometrical parameters (bond lengths and bond angles) calculated with HF and DFT methods using 6-311G basis set

have been compared with the corresponding ones as obtained by X-ray diffraction method and are presented in Table 2.

3.2.2. Molecular electrostatic potential (MEP)

The molecular electrostatic potential is a physically observable property that can be measured experimentally by diffraction approaches [40,41]. It is also used to illustrate the wide-ranging electronic and nuclear charge distribution, which is an appropriate feature for understanding the reactivity of various species [42]. The potential, $V(r)$, is typically written in terms of atomic units (a.u) and has the following form [43].

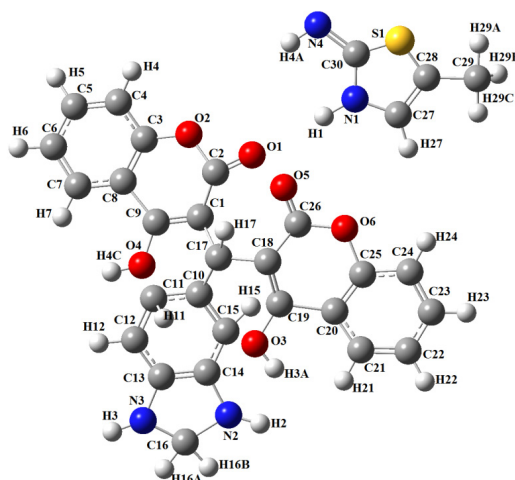


Figure 3. Optimized structure of 3,3'-[(3-benzimidazolyl)methylene]bis(4-hydroxy-2H-1-benzopyran-2-one):5-methyl-1,3-thiazol-2(3H)-imine.

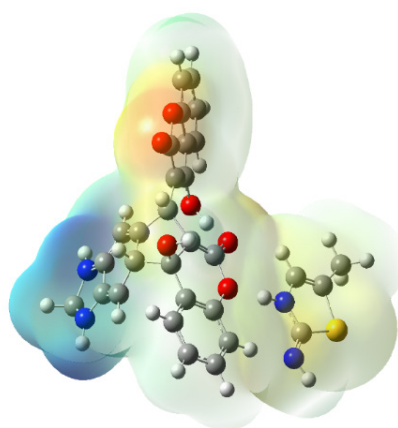


Figure 4. Molecular electrostatic potential map of 3,3'-[(3-benzimidazolyl)methylene]bis(4-hydroxy-2H-1-benzopyran-2-one):5-methyl-1,3-thiazol-2(3H)-imine.

$$V(r) = \sum_A \frac{Z_A}{|R_A - r|} - \int \frac{\rho(r')}{|r' - r|} d^3r' \quad (1)$$

where Z_A is the charge of the nucleus A located at R_A , $\rho(r')$ is the electronic density function of the molecule, and r' is the dummy integration variable.

MEP has been constructed using DFT/6-311G level of theory for 3, 3'-[(3-benzimidazolyl)methylene] bis(4-hydroxy-2H-1-benzopyran-2-one): 5-methyl-1, 3-thiazol-2(3H)-imine and is shown in Figure 4. In the color scheme of MEPs, red represents the electron rich, partially negative charge which is the preferred site for electrophilic attack, blue corresponds to electron deficient, partially positive charge which is the preferred site for nucleophilic attack, yellow for slightly electron rich region; green for neutral respectively. The color code of 3,3'-[(3-benzimidazolyl)methylene]bis(4-hydroxy-2H-1-benzopyran-2-one) : 5-methyl-1,3-thiazol-2(3H)-imine is in the range between -9.703×10^{-2} (deepest red) to 9.703×10^{-2} (deepest blue). It can be seen that the negative regions are mainly over the oxygen atoms and the positive potential sites are around the hydrogen atoms.

3.2.3. HOMO-LUMO analysis

The highest occupied molecular orbital (HOMO) and the lowest unoccupied molecular orbital (LUMO) are known as frontier molecular orbitals (FMOs). The FMOs plays an

important role in the optical and electrical properties as well as in quantum chemistry [44]. The HOMO represents electron-donating ability, while LUMO represents the electron accepting ability [45]. The pictorial representation of the energies of molecular orbitals is shown in Figure 5, the positive phase is represented by the red color and negative phase represented in green color). The HOMO lies at -4.82 eV and spreads over the thiazole ring whereas the LUMO is located at -3.36 eV which shows that the charge transfer to imidazole ring within the molecule and the energy gap is 1.46 eV. The energy difference between the HOMO and the LUMO orbital is called as energy gap that is important for the stability of structures. Both the HOMO and LUMO orbitals help describe the chemical reactivity and kinetic stability of the binary complex. By using HOMO and LUMO energy values for a molecule, the electronegativity and chemical hardness can be calculated as follows [46]:

$$\chi = -(E_{\text{HOMO}} + E_{\text{LUMO}})/2 = 4.09 \quad (2)$$

$$\eta = (E_{\text{LUMO}} - E_{\text{HOMO}})/2 = 0.73 \quad (3)$$

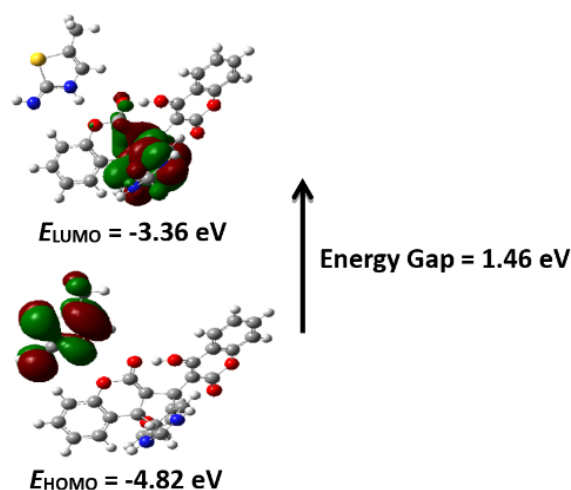
$$S = 1/2\eta = 0.68 \quad (4)$$

$$I = -E_{\text{HOMO}} = 4.82 \quad (5)$$

$$A = -E_{\text{LUMO}} = 3.36 \quad (6)$$

Table 4. HOMO-LUMO and other related molecular properties of 3,3'-[(3-benzimidazolyl)methylene]bis(4-hydroxy-2H-1-benzopyran-2-one):5-methyl-1,3-thiazol-2(3H)-imine.

Molecular parameters (eV)	B3LYP/6-311G
E_{LUMO}	-3.36
E_{HOMO}	-4.82
$E_{LUMO} - E_{HOMO}$	1.46
Ionization potential (I)	3.36
Electron affinity (A)	4.82
Electronegativity (χ)	4.09
Global hardness (η)	0.73
Chemical potential (μ)	-4.09
Global Electrophilicity (ω)	2.04

**Figure 5.** HOMO-LUMO plot of 3,3'-[(3-benzimidazolyl)methylene]bis(4-hydroxy-2H-1-benzopyran-2-one):5-methyl-1,3-thiazol-2(3H)-imine.

The HOMO and LUMO energies, the energy gap (ΔE), the ionization potential (I), the electron affinity (A), global hardness (η), chemical potential (μ), global electrophilicity (ω) for the investigated binary complex have been calculated at DFT/6-311G level and the results are given in Table 4.

3.2.4. Atomic net charges

The charge distribution on the molecule has an important influence on the vibrational spectrum. The total atomic charges of 3, 3'-[(3-benzimidazolyl)methylene] bis(4-hydroxy-2H-1-benzopyran-2-one): 5-methyl-1, 3-thiazol-2(3H)-imine obtained by Mulliken [47] methods using HF/6-311G and B3LYP/6-311G level of theory are shown in Table 5.

The atomic Mulliken charge values have been obtained by the Mulliken population analysis. It is based on the linear combination of atomic orbitals and therefore the wave function of the molecule. The range of hydrogen atom charge in the case of HF/6-311G is from 0.161 to 0.488, whereas the range of hydrogen atom charges in the case of B3LYP/6-311G(d,p) is from 0.149 to 0.432. All hydrogen atoms exhibit positive charge, which is an acceptor atom. The charge distribution for the oxygen atoms (O1, O2, O3, O4, O5, and O6) and nitrogen atoms (N1, N2, N3, and N4) present in the molecule have negative charge values which are donor atoms and their magnitudes decrease as we go from HF to DFT level of theory whereas sulphur atom has positive charge both in HF and DFT theory which is an acceptor atom.

3.2.5. Natural bond orbital analysis

Natural bond analysis provides an efficient method for studying intra- and inter-molecular bonding interactions among bonds and provides a convenient source for investigating charge transfer or conjugative interactions in molecular systems. It gives useful information about interactions in both

filled virtual orbital spaces which could enhance the analysis of intra- and inter-molecular interactions [48]. The natural bond orbital (NBO) calculation was performed using NBO program implemented in the Gaussian 09 package at the DFT/B3LYP level in order to understand various second-order interactions between the filled orbitals of one subsystem and vacant orbitals of another subsystem, which is a measure of the delocalization or hyperconjugation. The hyperconjugative interaction energy was deduced from the second-order perturbation approach [49]. For each donor NBO (i) and acceptor NBO (j), the stabilization energy $E(2)$ associated with electron delocalization between donor and acceptor is estimated as

$$E(2) = \Delta E_{ij} = q_i \frac{F(i,j)^2}{E_j - E_i} \quad (7)$$

where q_i is the donor orbital occupancy, E_i, E_j are diagonal elements (orbital energies), and $F(i,j)$ is the off-diagonal NBO Fock matrix element.

Larger the $E(2)$ value, the more intensive is the interaction between the electron donor and electron acceptor, i.e., the more donating tendency from the electron donor to electron acceptors and the extent of electron delocalization is greater. The results of second-order perturbation theory analysis of Fock matrix at B3LYP/6-311G level of theory are collected in Table 6.

In this compound, the strong intra-molecular hyperconjugation interaction of the π electrons from C18-C19 to the π^* antibonding orbitals of C26-O5 and σ (C6-C5) to the σ^* antibonding orbital C8-C7 leads to the stabilization energy of 30.36 and 23.44 kJ/mol, respectively. The most important interaction energy related to the resonance in the binary complex is the electron donating from the lone pair LP O1 atom to σ^* (C1-C2) and LP N3 atom to σ^* (C13-C12) which leads to a stabilization energy of 56.98 and 39.65 kJ/mol, respectively.

Table 5. Mulliken charges using HF and DFT theory.

Atom no	Mulliken (HF/6-311G)	Mulliken (B3LYP/6-311G)
C13	0.251087	0.314476
C14	0.485383	0.258599
C15	-0.039955	0.049746
C10	0.287460	0.103562
C11	-0.438188	-0.320469
C12	0.110025	0.055399
H15	0.225850	0.211357
H12	0.215910	0.190972
N3	-0.946875	-0.820857
N2	-0.964970	-0.774947
C16	0.182368	0.069975
H3	0.361921	0.348392
H2	0.399899	0.368059
H16B	0.210958	0.217518
H16A	0.208974	0.220085
C17	-0.493542	-0.480255
C1	-0.084671	0.018405
C2	0.820503	0.583461
C9	0.094619	-0.071655
C8	0.021775	0.037947
C3	0.305067	0.236978
H11	0.297138	0.268804
O2	-0.789026	-0.616687
O1	-0.797180	-0.596030
O4	-0.738375	-0.591135
H4C	0.408051	0.368489
C7	-0.149051	-0.113887
C6	-0.175219	-0.157784
C5	-0.157243	-0.151340
C4	-0.182099	-0.162701
H7	0.178553	0.161375
H6	0.161152	0.147715
H5	0.164646	0.149822
H4	0.289050	0.249553
C18	-0.233884	-0.105957
C26	0.743513	0.496077
C19	0.616685	0.388833
C20	-0.213317	-0.156950
C25	0.387685	0.289643
O6	-0.687697	-0.509336
H17	0.309773	0.265387
O5	-0.514493	-0.371347
C21	-0.079446	-0.068824
C22	-0.187771	-0.165099
C24	-0.191184	-0.163029
C23	-0.103081	-0.110996
H21	0.213159	0.183199
H22	0.169470	0.153234
H23	0.170681	0.154871
H24	0.201202	0.180110
O3	-0.819505	-0.633236
H3A	0.488926	0.398229
C28	-0.409296	-0.380254
C27	0.382935	0.317406
C30	0.368787	0.216696
N1	-0.866889	-0.704579
S1	0.192235	0.200104
C29	-0.568555	-0.595302
N4	-0.670799	-0.546805
H29C	0.187736	0.192695
H29A	0.188584	0.192440
H29B	0.190970	0.196152
H4A	0.264622	0.254694
H1	0.485942	0.432944
H27	0.259014	0.226059

3.2.6. Fukui function

Density Functional Theory is a powerful tool for the study of reactivity and selectivity in a molecule [50]. The most basic and commonly used local reactivity parameter is the Fukui function, which indicates the tendency of the electron density to deform at a given position upon accepting or donating electrons [51,52]. Fukui function gives us information about the electrophilic/nucleophilic power of a given atomic site in a molecule. The condensed Fukui functions on the j^{th} atom site can be expressed as:

$$f_j^+ = q_j(N+1) - q_j(N) \quad (8)$$

$$f_j^0 = \frac{1}{2}[q_j(N+1) - q_j(N-1)] \quad (9)$$

$$f_j^- = q_j(N) - q_j(N-1) \quad (10)$$

where f_j^+ for nucleophilic attack, f_j^- for electrophilic attack and f_j^0 for free radical. In these equations, q_j is the atomic charge at the j^{th} atomic site in the neutral (N), anionic (N+1), or cationic (N-1) chemical species.

Table 6. Second-order perturbation theory analysis of Fock matrix of 3,3'-[(3-benzimidazolyl)methylene]bis(4-hydroxy-2H-1-benzopyran-2-one):5-methyl-1,3-thiazol-2(3H)-imine by NBO method at B3LYP/6-311G(d,p) level.

Donor (i)	ED(i)(e)	Acceptor (j)	ED(j)(e)	E(2) (KJ/mol) ^a	E(j) - E(i) (a.u) ^b	F(i,j) (a.u) ^c
σ (C13-C14)	1.96134	σ* (C14-C15)	0.02290	3.07	1.21	0.055
σ (C13-C14)	1.96134	σ* (N2-H2)	0.01427	4.44	1.06	0.062
σ (C13-C12)	1.97402	σ* (C13-C14)	0.03863	4.61	1.18	0.066
σ (C13-N3)	1.98467	σ* (C13-C12)	0.01793	3.99	1.43	0.068
σ (C14-C15)	1.97009	σ* (C15-C10)	0.02433	4.33	1.31	0.067
σ (C15-C10)	1.97414	σ* (C14-N2)	0.02208	5.27	1.18	0.070
σ (C15-H15)	1.97052	σ* (C10-C11)	0.02635	5.98	0.92	0.066
σ (C17-C1)	1.92065	σ* (C15-C10)	0.18601	8.82	0.58	0.065
σ (C1-C2)	1.84116	σ* (C9-O4)	0.08400	8.38	0.48	0.057
σ (C9-O4)	1.98372	σ* (C8-C3)	0.03647	1.11	1.34	0.034
σ (C8-C7)	1.66693	σ* (C3-C4)	0.37020	22.55	0.28	0.072
σ (C3-C4)	1.61133	σ* (C8-C7)	0.40517	22.43	0.28	0.070
σ (C6-C5)	1.64673	σ* (C8-C7)	0.40517	23.44	0.27	0.072
π (C18-C19)	1.76968	π* (C26-O5)	0.33748	30.36	0.26	0.082
σ (C26-O6)	1.99290	σ* (C18-C26)	0.05865	2.63	1.49	0.057
LP (1) N(3)	1.79677	σ* (C13-C12)	0.22058	39.65	0.30	0.098
LP (3) O(1)	1.68771	σ* (C1-C2)	0.34221	56.98	0.30	0.117
LP (2) O(5)	1.83576	σ* (C26-O6)	0.12214	37.44	0.50	0.124
LP (2) O(3)	1.83601	π* (C18-C19)	0.28696	18.84	0.39	0.079
σ* (C15-C10)	0.18601	σ* (C1-C2)	0.34221	9.73	0.03	0.028
σ* (C8-C7)	0.40517	σ* (C9-O4)	0.08400	4.62	0.18	0.052
π* (C26-O5)	0.33748	π* (C18-C19)	0.28696	72.06	0.03	0.075
σ* (C20-C25)	0.42731	σ* (C21-C22)	0.29231	236.10	0.01	0.080

^a E(2) means energy of hyperconjugative interactions.^b Energy difference between donor and acceptor i and j NBO orbitals.^c F(i,j) is the Fock matrix element between i and j NBO orbitals.**Table 7.** Fukui indices for nucleophilic and electrophilic attacks on atoms calculated from natural population analysis at DFT-B3LYP/6-311G.

Atom	F _s ⁺	F _s ⁻	Δf(r)
C13	0.00937	-0.02345	0.03282
C14	0.00770	0.17867	-0.17097
C15	0.01838	-0.02978	0.04816
C10	-0.00923	0.18086	-0.19009
C11	0.00155	-0.03583	0.03738
C12	-0.00392	0.11262	-0.11654
H15	0.00865	0.03557	-0.02692
H12	0.00621	0.03251	-0.02630
N3	0.01043	0.01413	-0.00370
N2	0.02034	0.07698	-0.05664
H3	0.00775	0.02548	-0.01773
H2	0.00862	0.03421	-0.02559
C17	-0.01082	-0.00694	-0.00388
C1	0.13197	0.00373	0.12824
C2	-0.00424	0.02333	-0.02757
C9	-0.01389	0.01428	-0.02817
O2	0.00736	0.01525	-0.00789
O1	0.04897	0.04419	0.00478
O4	0.02437	0.00377	0.02060
C26	0.00096	0.00381	-0.00285
C19	0.00509	0.01274	-0.00765
O6	0.01021	0.01182	-0.00161
O5	0.01342	0.00746	0.00596
O3	0.00191	-0.00265	0.00456
N1	0.06728	-0.00373	0.07101
S1	0.14188	0.02853	0.11335
N4	0.13501	-0.01195	0.14696
H4A	0.02133	0.00729	0.01404
H1	0.01244	-0.01152	0.02396

The atomic charges either calculated by natural population analysis (NPA) or by Mulliken population analysis (MPA) have been used to calculate the Fukui function. In the present study the values of Fukui Function calculated from the NBO charges. The dual descriptor Δf(r) [53] for the calculation of nucleophilicity and electrophilicity is defined as the difference between the nucleophilic and electrophilic Fukui functions and is given by the Equation (11):

$$\Delta f(r) = f_j^+ - f_j^- \quad (11)$$

If Δf(r) > 0, then the site is favored for nucleophilic attack, whereas if Δf(r) < 0, then the site is favored for an electrophilic attack. According to the dual descriptor, Δf(r) gives a transparent distinction between nucleophilic and electrophilic attacks at a particular site with their sign. From the values

reported in Table 7, according to the condition for dual descriptor, nucleophilic site in our title molecule is C1, C13, C15, C11, O1, O3, O4, O5, N1, N4, S1, H4A and H1 are positive values (i.e. Δf(r) > 0). Similarly, the electrophilic site is C10, C12, C14, C2, C9, C19, C26, C17, N2, N3, O2, O6, H2, H3, H12 and H15 negative values (i.e. Δf(r) < 0).

4. Conclusion

In this present investigation, the synthesis and the molecular structure analysis of 3,3'-[(3-benzimidazolyl)methylene]bis(4-hydroxy-2H-1-benzopyran-2-one):5-methyl-1,3-thiazol-2(3H)-imine has been reported by X-ray crystallographic techniques and NBO, HOMO-LUMO, Fukui function, atomic net charge analysis by HF and DFT-B3LYP methods at 6-311G basis set. In the crystal structure, the presence of coumarine and 5-methyl-1,3-thiazol-2(3H)-imine promotes the formation of

intermolecular hydrogen bond network. The molecular packing in the unit cell is stabilized via N-H...O and C-H...N intermolecular interactions. The computed geometric parameters (bond length, bond angle) have been compared with their corresponding experimental data. The molecular electrostatic potential map indicates that the negative potential sites are on electronegative atoms and the positive potential sites are around the hydrogen atoms. These sites provide information concerning the region from where the structure may result into the formation of intra- and intermolecular interactions.

Acknowledgements

Rajni Kant acknowledges the Research Grants as sanctioned under Rashtriya Uchcharat Shiksha Abhiyan (RUSA) 2.0 Project (Ref. No: RUSA/JU/2/2019-20/111/3588-3636).

Supporting information

CCDC-1948179 contains the supplementary crystallographic data for this paper. These data can be obtained free of charge via <https://www.ccdc.cam.ac.uk/structures/>, or by e-mailing data_request@ccdc.cam.ac.uk, or by contacting The Cambridge Crystallographic Data Centre, 12 Union Road, Cambridge CB2 1EZ, UK; fax: +44(0)1223-336033.

Disclosure statement

Conflict of interest: The authors declare that they have no conflict of interest.

Author contributions: All authors contributed equally to this work.

Ethical approval: All ethical guidelines have been adhered.

Sample availability: Samples of the compounds are available from the author.

ORCID

Gopal Sharma

 <http://orcid.org/0000-0003-4780-2804>


Anshul Uppal

 <http://orcid.org/0000-0001-8203-616X>


Sumati Anthal

 <http://orcid.org/0000-0001-7947-7335>

Madhukar Baburao Deshmukh

 <http://orcid.org/0000-0001-7097-2356>

Priyanka Pandharinath Mohire

 <http://orcid.org/0000-0003-4644-1111>

Tanaji Ramchandra Bhosale

 <http://orcid.org/0000-0002-0372-7702>

Chellappanpillai Sudarsanakumar

 <http://orcid.org/0000-0003-2750-7795>

Rajni Kant

 <http://orcid.org/0000-0001-8043-2329>

References

- [1]. Kontogiorgis, C.; Detsi, A.; Hadjipavlou-Litina, D. *Exp. Opin. Therap. Pat.* **2012**, *22*, 437-454.
- [2]. Kostova, I. *Curr. Med. Chem. Anti-Cancer Agents* **2005**, *5*, 29-46.
- [3]. Weinmann, I. *Coumarins: Biology, Applications and Mode of Action*, John Wiley & Sons, USA, 1997, pp. 1-22.
- [4]. Saeed, A.; Ashraf, S.; Florke, U.; Delgado Espinoza, Z. Y.; Erben, M. F.; Perez, H. J. *Mol. Struct.* **2016**, *1111*, 76-83.
- [5]. Wang, K.; Liu, Z.; Guan, R.; Cao, D.; Chen, H.; Shan, Y.; Wu, Q.; Xu, Y. *Spectrochim. Acta A* **2015**, *144*, 235-242.
- [6]. Perez-Cruz, F.; Vazquez-Rodriguez, S.; Matos, M. J.; Herrera-Morales, A.; Villamena, F. A.; Das, A.; Gopalakrishnan, B.; Olea-Azar, C.; Santana, L.; Uriarte, E. *J. Med. Chem.* **2013**, *56*, 6136-6145.
- [7]. Saeed, A.; Zaib, S.; Ashraf, S.; Iftikhar, J.; Muddassar, M.; Zhang, K. Y. J.; Iqbal, J. *Bioorg. Chem.* **2015**, *63*, 58-63.

- [8]. Medina, F. G.; Marrero, J. G.; Macias-Alonso, M.; Gonzalez, M. C.; Cordova-Guerrero, I.; Teissier Garcia, A. G.; Osegueda-Robles, S. *Nat. Prod. Rep.* **2015**, *32*, 1472-1507.
- [9]. Smyth, T.; Ramachandran, V. N.; Smyth, W. F. *Int. J. Antimicrob. Agents* **2009**, *33*, 421-426.
- [10]. Manvar, A.; Malde, A.; Verma, J.; Virsodia, V.; Mishra, A.; Upadhyay, K.; Acharya, H.; Coutinho, E.; Shah, A. *Eur. J. Med. Chem.* **2008**, *43*, 2395-2403.
- [11]. Belluti, F.; Fontana, G.; Dal Bo, L.; Carenini, N.; Giommarelli, C.; Zunino, F. *Bioorg. Med. Chem.* **2010**, *18*, 3543-3550.
- [12]. Yu, D.; Suzuki, M.; Xie, L.; Morris-Natschke, S. L.; Lee, K. H. *Med. Res. Rev.* **2003**, *23*, 322-345.
- [13]. Kalkhambkar, R. G.; Kulkarni, G. M.; Kamanavalli, C. M.; Premkumar, N.; Asdaq, S. M. B.; Sun, C. M. *Eur. J. Med. Chem.* **2008**, *43*, 2178-2188.
- [14]. Keri, R. S.; Hosamani, K. M.; Shingalapur, R. V.; Hugar, M. H. *Eur. J. Med. Chem.* **2010**, *45*, 2597-2605.
- [15]. Wood, W. J.; Patterson, A. W.; Tsuruoka, H.; Jain, R. K.; Ellman, J. A. *J. Am. Chem. Soc.* **2005**, *127*, 15521-15527.
- [16]. Sashidhara, K. V.; Kumar, A.; Kumar, M.; Sarkar, J.; Sinha, S.; *Bioorg. Med. Chem. Lett.* **2010**, *20*, 7205-7211.
- [17]. Radanyi, C.; Le Bras, G. L.; Messaoudi, S.; Bouclier, C. L.; Peyrat, J. F. o.; Brion, J. D.; Marsaud, V. r.; Renoir, J. M.; Alami, M. d.; *Bioorg. Med. Chem. Lett.* **2008**, *18*, 2495-2498.
- [18]. Chimenti, F.; Secci, D.; Bolasco, A.; Chimenti, P.; Granese, A.; Befani, O.; Turini, P.; Alcaro, S.; Ortuso, F. *Bioorg. Med. Chem. Lett.* **2004**, *14*, 3697-3703.
- [19]. Nolan, A. K.; Doncaster, R. J.; Dunstan, S. M.; Scot, A. K.; Frenkel, D.; Siegel, D.; Ross, D.; Barnes, J.; Levy, C.; Leys D. *J. Med. Chem.* **2009**, *57*, 7142-7156.
- [20]. Mahajan, D. H.; Pannecouque, C.; De Clercq, E.; Chikhalia, K. H. *Arch. Pharm.* **2009**, *342*, 281-290.
- [21]. Zhao, H.; Neamati, N.; Hong, H.; Mazumder, A.; Wang, S.; Sunder, S.; Milne, G. W. A.; Pommier, Y.; Burke, T. R. *J. Med. Chem.* **1997**, *40*, 242-249.
- [22]. Saeed, A.; Arif, M.; Erben, M. F.; Florke, U.; Simpson, J. *Spectrochim. Acta A* **2018**, *198*, 290-296.
- [23]. Luo, Y.; Yao, J.; Yang, L.; Feng, C.; Tang, W.; Wang, G.; Zuo, J.; Lu, W. *Arch. Pharm. Chem. Life Sci.* **2011**, *2*, 78-83.
- [24]. Arjmand, F.; Aziz, M. *Eur. J. Med. Chem.* **2009**, *44*, 834-844.
- [25]. Osman, H.; Arshad, A.; Lam, C. K.; Bagley, M. C. *Chem. Cent. J.* **2012**, *6*, 32-42.
- [26]. Bruker (2009). SADABS. Bruker AXS Inc., Madison, Wisconsin, USA.
- [27]. Sheldrick, G. M. *Acta Cryst. A* **2008**, *64*, 112-122.
- [28]. Sheldrick, G. M. *Acta Cryst. C* **2015**, *71*, 3-8.
- [29]. Farrugia, L. J. *J. Appl. Cryst.* **2012**, *45*, 849-854.
- [30]. Nardelli, M. J. *J. Appl. Cryst.* **1995**, *28*, 659-659.
- [31]. Spek, A. L. *Acta Cryst. D* **2009**, *65*, 148-155.
- [32]. Becke, A. D. *J. Chem. Phys.* **1993**, *98*, 5648-5652.
- [33]. Becke, A. D. *Phys. Rev. A* **1988**, *38*, 3098-3100.
- [34]. Lee, C. T.; Yang, W. T.; Parr, R. G. *Phys. Rev. B* **1988**, *37*, 785-789.
- [35]. Frisch, M. J.; Trucks, G. W.; Schlegel, H. B.; Scuseria, G. E.; Robb, M. A.; Cheeseman, J. R.; Montgomery, Jr., J. A.; Vreven, T.; Kudin, K. N.; Burant, J. C.; Millam, J. M.; Iyengar, S. S.; Tomasi, J.; Barone, V.; Mennucci, B.; Cossi, M.; Scalmani, G.; Rega, N.; Petersson, G. A.; Nakatsuji, H.; Hada, M.; Ehara, M.; Toyota, K.; Fukuda, R.; Hasegawa, J.; Ishida, M.; Nakajima, T.; Honda, Y.; Kitao, O.; Nakai, H.; Klene, M.; Li, X.; Knox, J. E.; P. Hratchian, H.; Cross, J. B.; Adamo, C.; Jaramillo, J.; Gomperts, R.; Stratmann, R. E.; Yazyev, O.; Austin, A. J.; Cammi, R.; Pomelli, C.; Ochterski, J. W.; Ayala, P. Y.; Morokuma, K.; Voth, G. A.; Salvador, P.; Dannenberg, J. J.; Zakrzewski, V. G.; Dapprich, S.; Daniels, A. D.; Strain, M. C.; Farkas, O.; Malick, D. K.; Rabuck, A. D.; Raghavachari, K.; Foresman, J. B.; Ortiz, J. V.; Cui, Q.; Baboul, A. G.; Clifford, S.; Cioslowski, J.; Stefanov, B. B.; Liu, G.; Liashenko, A.; Piskorz, P.; Komaromi, I.; Martin, R. L.; Fox, D. J.; Keith, T.; AlLaham, M. A.; Peng, C. Y.; Nanayakkara, A.; Challacombe, M.; Gill, P. M. W.; Johnson, B.; Chen, W.; Wong, M. W.; Gonzalez, C.; Pople, J. A. et al. , Gaussian 09, Revision A. 02, Gaussian, Inc. , Wallingford CT, 2009.
- [36]. Macrae, C. F.; Bruno, I. J.; Chisholm, J. A.; Edgington, P. R.; McCabe, P.; Pidcock, E.; Rodriguez-Monge, L.; Taylor, R.; van de Streek, J.; Wood, P. A. *J. Appl. Cryst.* **2008**, *41*, 466-470.
- [37]. Allen, F. H.; Kennard, O.; Watson, D. G.; Brammer, L.; Orpen, A. G.; Taylor, R. *J. Chem. Soc. Perk. T. 2* **1987**, 1-19.
- [38]. Manolov, I.; Morgenstern, B.; Hegetschweiler, K. *X-ray Struct. Anal. Online* **2012**, *28*, 83-84.
- [39]. Dochev, S.; Roller, A.; Milunovic, M.; Manolov, I. *X-ray Struct. Anal. Online* **2017**, *33*, 53-54.
- [40]. Politzer, P.; Truhlar, D. G. *Chemical Applications of Atomic and Molecular Electrostatic Potentials*, New York: Plenum Press, 1981.
- [41]. Stewart, R. F. *Chem. Phys. Lett.* **1979**, *65*, 335-342.
- [42]. Murray, J. S.; Politzer, P. *WIREs Comput. Mol. Sci.* **2011**, *1*, 153-163.
- [43]. Politzer, P.; Murray, J. S. *Theoret. Chem. Accounts* **2002**, *108*, 134-142.
- [44]. Joshi, B. D.; Mishra, R.; Tandon, P.; Oliveira, A. C.; Ayala, A. P. *J. Mol. Struct.* **2014**, *1058*, 31-40.
- [45]. Munoz-Caro, C.; Nino, A.; Sement, M. L.; Leal, J. M.; Ibeas, S. *J. Org. Chem.* **2000**, *65*, 405-410.

- [46]. Pearson, R. G. *Proceed. Nat. Acad. Sci. USA* **1986**, *83*, 8440-8841.
[47]. Mulliken, R. S. *J. Chem. Phys.* **1955**, *23*, 1833-1840.
[48]. Choo, J.; Kim, S.; Joo, H.; Kwon, Y. *J. Mol. Struct.* **2002**, *587*, 1-8.
[49]. Reed, A. E.; Curtiss, L. A.; Weinhold, F. *Chem. Rev.* **1988**, *88*, 899-926.
[50]. Parr, R. G.; Yang, W. *Density Functional Theory of Atoms and Molecules*, Oxford University Press, New York, 1989.
[51]. Ayers, P. W.; Parr, R. G. *J. Am. Chem. Soc.* **2000**, *122*, 2010-2018.
[52]. Parr, R. G.; Yang, W. *J. Am. Chem. Soc.* **1984**, *106*, 511-516.
[53]. Morell, C.; Grand, A.; Toro-Labbe, A. *J. Phys. Chem.* **2005**, *109*, 205-212.



Copyright © 2020 by Authors. This work is published and licensed by Atlanta Publishing House LLC, Atlanta, GA, USA. The full terms of this license are available at <http://www.eurjchem.com/index.php/eurjchem/pages/view/terms> and incorporate the Creative Commons Attribution-Non Commercial (CC BY NC) (International, v4.0) License (<http://creativecommons.org/licenses/by-nc/4.0>). By accessing the work, you hereby accept the Terms. This is an open access article distributed under the terms and conditions of the CC BY NC License, which permits unrestricted non-commercial use, distribution, and reproduction in any medium, provided the original work is properly cited without any further permission from Atlanta Publishing House LLC (European Journal of Chemistry). No use, distribution or reproduction is permitted which does not comply with these terms. Permissions for commercial use of this work beyond the scope of the License (<http://www.eurjchem.com/index.php/eurjchem/pages/view/terms>) are administered by Atlanta Publishing House LLC (European Journal of Chemistry).